Pre-Teide Volcanic Activity on the Northeast Volcanic Rift Zone

5

Valentin R. Troll, Frances M. Deegan, Audray Delcamp, Juan Carlos Carracedo, Chris Harris, Benjamin van Wyk de Vries, Michael S. Petronis, Francisco J. Perez-Torrado, Jane P. Chadwick, Abigail K. Barker, and Sebastian Wiesmaier

Abstract

The northeast rift zone of Tenerife (NERZ) presents a partially eroded volcanic rift that offers a superb opportunity to study the structure and evolution of oceanic rift zones. Field data, structural observations,

V. R. Troll (✉) · F. M. Deegan · A. K. Barker
Department of Earth Sciences (CEMPEG), Uppsala
University, Uppsala 75236, Sweden
e-mail: Valentin.Troll@geo.uu.se

F. M. Deegan
Laboratory for Isotope Geology, Swedish Museum
of Natural History, Stockholm, Sweden

A. Delcamp
Department of Geography, Vrije Universiteit
Brussels, Brussels 1050, Belgium

J. C. Carracedo · F. J. Perez-Torrado
Departamento de Física (GEOVOL), Universidad de
Las Palmas de Gran Canaria, Las Palmas de Gran
Canaria, Canary, Islands, Spain

C. Harris
Department of Geological Sciences, University of
Cape Town, Rondebosch 7701, South Africa

B. van Wyk de Vries
Laboratoire Magmas et Volcans, Université Blaise
Pascal, Clermont, Ferrand, France

M. S. Petronis
Environmental Geology Natural Resource
Management Department, New Mexico Highlands
University, Las Vegas, New Mexico 87701, U.S.A

J. P. Chadwick
Science Gallery, Trinity College Dublin, Dublin 2,
Ireland

S. Wiesmaier
Department of Earth and Environmental Sciences,
Ludwig-Maximilians Universität (LMU), Munich,
Germany

isotopic dating, magnetic stratigraphy, and isotope geochemistry have recently become available for this rift and provide a reliable temporal framework for understanding the structural and petrological evolution of the entire rift zone. The NERZ appears to have formed in several major pulses of activity with a particularly high production rate in the Pleistocene (ca. 0.99 and 0.56 Ma). The rift underwent several episodes of flank creep and eventual catastrophic collapses driven by intense intrusive activity and gravitational adjustment. Petrologically, a variety of mafic rock types, including crystal-rich ankaramites, have been documented, with most samples isotopically typical of the "Tenerife signal". Some of the NERZ magmas also bear witness to contamination by hydrothermally altered components of the island edifice and/or sediments. Isotope geochemistry furthermore points to the generation of the NERZ magmas from an upwelling column of mantle plume material mixed with upper asthenospheric mantle. Finally, persistent isotopic similarity through time between the NERZ and the older central edifices on Tenerife provides strong evidence for a genetic link between Tenerife's principal volcanic episodes.

5.1   Ocean Island Rift Zones

Rift zones on ocean islands such as the Canary, Hawaiian, and Cape Verde archipelagos are major volcanic surface alignments associated with intense dyke intrusions at depth. Volcanic rift zones are extremely important in terms of Ocean Island growth and evolution as discussed by Carracedo and Troll in Chap. 4. Firstly, rift zones generally form prominent, major topographical features on ocean islands as they concentrate volcanic activity, and thus control the distribution of both volcanic hazards and natural resources. On Tenerife (Fig. 5.1), for example, access to fresh groundwater is aided by water tunnels (galerías) constructed into the rift zone's interior (Navarro and Farrujia 1989). Finally, and perhaps most importantly, Ocean Island rift zones control the structure of a growing volcanic edifice, perhaps even from their initial stages of growth, and thus define the location of large-scale flank collapses, which are particularly prominent on Tenerife (e.g., Carracedo 1994; Walter and Troll 2003; Carracedo et al. 2011; see also Fig. 5.1).

Ocean Island rift zones were initially recognised and described on the Hawaiian Islands (Fiske and Jackson 1972; Swanson et al. 1976; Walker 1986, 1987, 1992; Dieterich 1988). Perhaps the most significant progress in understanding Ocean Island rift zone genesis and structural development has been made through their study in the Canary Islands (e.g., Carracedo 1975, 1979, 1994, 1996, 1999; Carracedo et al. 1992, 1998, 2001, 2007, 2011; Guillou et al. 1996; Walter and Schmincke 2002; Walter and Troll 2003; Walter et al. 2005; Hansen 2009; Delcamp et al. 2010, 2012; Carracedo and Troll, this volume). The Canary Islands as a whole are especially valuable to the study of rift zone development due to the fact that the rifts are generally long-lived, dynamic, and conspicuously large structures. The combination of relatively low plume activity feeding the Canaries, low velocity of the African Plate in comparison to, e.g., the Pacific Plate that underlies the Hawaiian Islands, and a prolonged subaerial volcanic history with the absence of late subsidence, gives rise to long-lived ridges on the Canary Islands that are prone to frequent recurring volcanic activity and also to recurring volcanic failure (see Chap. 4 for further discussion). Hence, the spatial circumstances particular to the Canary archipelago provide us with an outstanding and unique opportunity to investigate rift processes in immense detail and with as yet unparalleled temporal resolution.
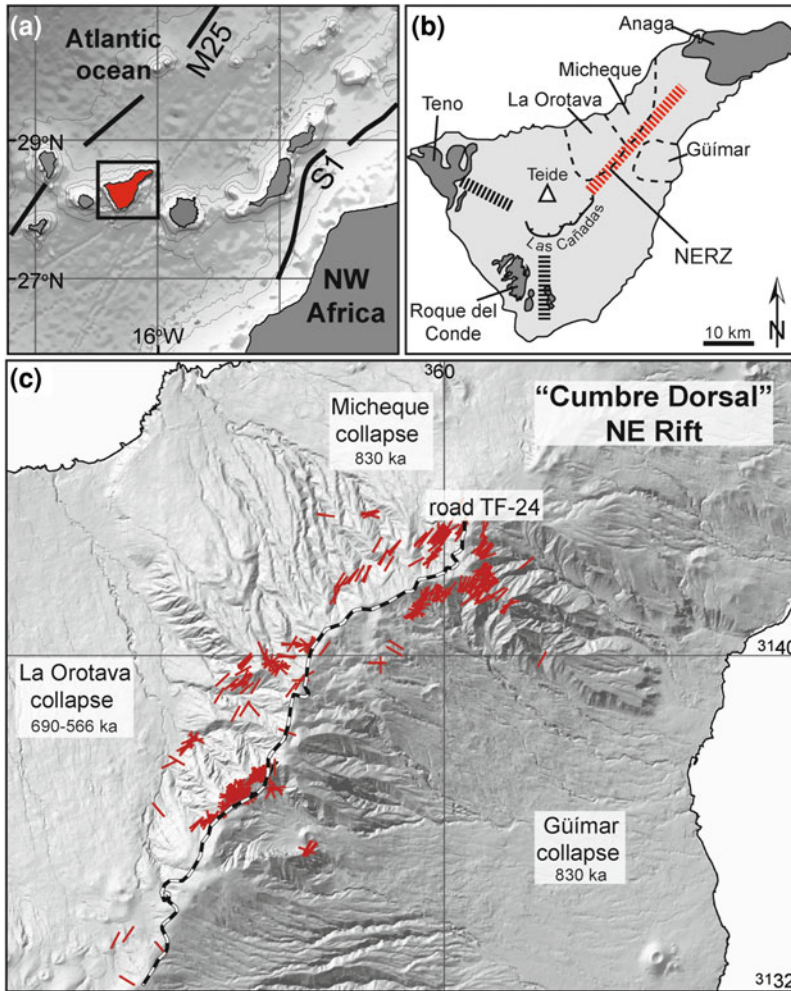
Fig. 5.1 a Map of the Canary Archipelago, located off the coast of NW Africa between magnetic anomalies S1 (175 Ma) and M25 (156 Ma) (Roeser 1982) with Tenerife highlighted. **b** Simplified geological map of Tenerife showing *1* the location of the shield basalt massifs Roque del Conde (the Central Shield), as well as Teno, and Anaga, *2* the three rift zones (*thick dashed black* and *red lines*) and the collapse scars flanking the NERZ, *3* the Las Cañadas caldera wall, and *4* the location of the Teide Volcanic Complex at the junction of the three rift zones. **c** Shaded relief map of the NERZ showing the distribution of the investigated dykes along the rift (*short red lines*) and the three collapse depressions flanking the ridge. The *thick black* and *white line* is the main road TF-24, along which there is good exposure of the NERZ dykes (see Fig. 5.2b). (Image adapted after Deegan et al. 2012)

5.2 Geology of the NERZ and Research Developments

Various intervals of rift zone development are represented in the Canary Islands. For instance, the rifts of the younger western islands El Hierro and La Palma are characteristic of the shield development stage. The NW and NE rifts on Tenerife, on the other hand, represent part of the more advanced, post-erosional (rejuvenation) stage of island growth (see Carracedo and Pérez-Torrado, Chap. 2). The NERZ (Fig. 5.1) has been largely inactive for thousands of years along most of its length with only a single known historic eruption in 1704–1705 A.D., which produced relatively small volumes of lava ($<3.5 \times 10^6$ m; Carracedo et al. 2006). The products of this eruption are
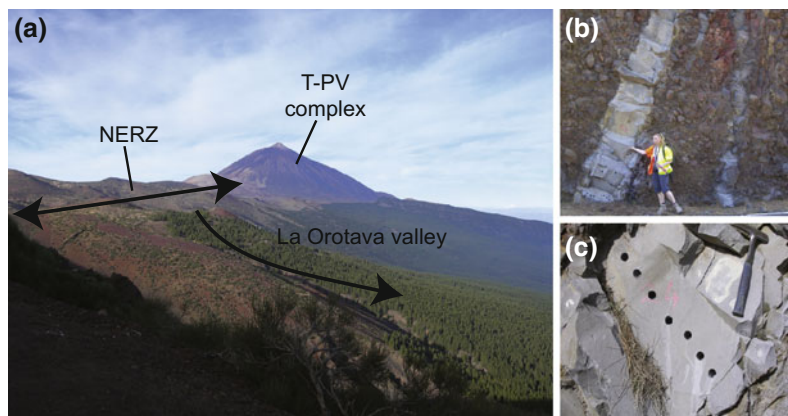
Fig. 5.2 a Photograph showing the roughly linear ridge of the Northeast rift zone (NERZ) of Tenerife, and the Teide-Pico Viejo (T-PV) complex, which sits at the south-westernmost projection of the NERZ. La Orotava collapse scar can be seen to the NW of the rift. **b** Field appearance of dykes intruded along the rift exposed along the main road TF-24. **c** Example of a dyke outcrop that has been drilled to retrieve fresh samples of the dyke interior for palaeomagnetic and geochemical studies (hammer to *top right* of image for scale)

restricted to the headwall of the Güímar landslide scar (the Arafo volcano), and probably do not reflect direct rift products themselves (cf. Longpré et al. 2009). The protracted inactivity, coupled with extensive erosion, and several giant landslide events on either side of the rift, has created a dissected anatomy of this oceanic rift system. This situation allows for in-depth study of the rift's internal structure, especially the complex network of dykes that would otherwise not be generally accessible, but which is available in the NERZ for high resolution structural and geochemical studies (Fig. 5.2) summarised in this chapter.

The NERZ is a ca. 30 km long ridge that extends from the central edifice of Las Cañadas at its SW end, to the Anaga massif at its NE termination (Fig. 5.1). The overall height of the NERZ decreases from the centre of the island to the northeast (e.g., Izaña, 2,386 m above sea level [asl]; Ayosa, 2,078 m asl; Joco, 1,956 m asl; Gaitero, 1,748 m asl). The ridge-like topography of the NERZ has been shaped by three successive mass wasting events along its flanks. From aerial view, these landslide scars can be seen as depressions on both sides of the ridge (Fig. 5.1). The Micheque and Güímar landslides were roughly coeval, taking place at ca. 0.83 Ma, while the more recent La Orotava landslide occurred at 0.56 Ma (Figs. 5.1 and 5.2; Carracedo et al. 2011 and references therein).

Although the NERZ is one of the pronounced geological features on Tenerife, its challenging complexity has prevented intense study so far. Recent research efforts to unravel the complexity of the NERZ involved systematic and in-depth mapping of the rift; structural analysis of over 400 dykes, including dykes exposed within the Micheque, Güímar, and La Orotava collapse scars and dykes in water tunnels (*galerías*); and investigations into dyke petrography, morphology, thickness, orientation, and their internal features (e.g., Fig. 5.3; Delcamp et al. 2010, 2012). High spatial resolution sampling of dykes along roadcuts and from *galerías* (see Fig. 5.1) has also been carried out for (1) thin-section preparation and petrographic analysis; (2) paleomagnetic measurements, with samples for this purpose collected using a portable gasoline powered drill (Fig. 5.2; full analytical details can be found in Delcamp et al. 2010); (3) $^{40}Ar/^{39}Ar$ age determination (see Delcamp et al. 2010); and (4) geochemical analysis, including major and trace elements of over 80 dyke samples following the method in Abratis et al. (2002). A sub-set of these 80 samples was analyzed for stable (oxygen) isotopes following the procedure given in Vennemann and Smith (1990) and Fagereng et al. (2008). Finally, a selection of these was further analysed for combined trace and rare earth element (REE) and Sr–Nd–Pb isotopes. Full analytical details, including measurements of internal and external standards, and the entire
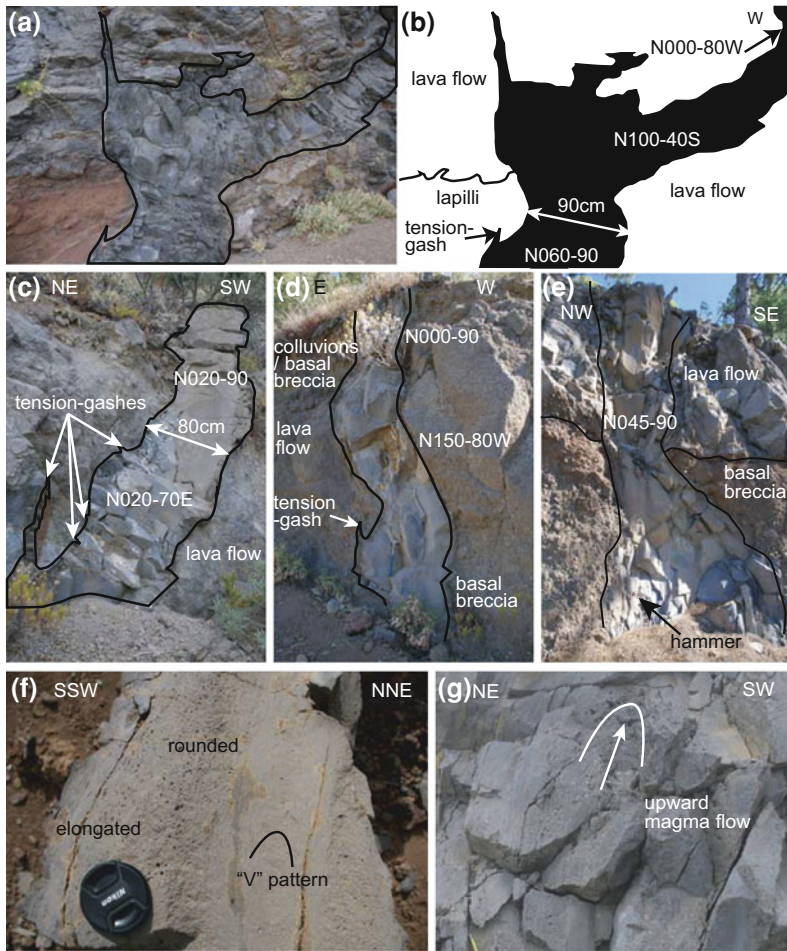
Fig. 5.3 Photographs of the field appearance of representative dykes of the NERZ with variations in orientation (strike, dip or both), thickness, and texture observed on the single intrusion scale. Images from Delcamp et al. (2012). **a**, **b** Dyke orientation is seen to change at the transition between surrounding lapilli and a lava flow. **c** Dyke showing a change in orientation within a lava flow unit. **d** Dyke showing a change in orientation at the transition between surrounding basal breccia and a lava flow. **e** Variation in dyke thickness due to a change in the host-rock lithology. The dyke is thicker within the basal breccia (lower part, low competence layer) than within the lava flow (upper part, high competence layer). **f** Example of vesicle types and distribution in a dyke interior. **g** Example showing the direction of magma flow as recorded by vesicle orientation

geochemical data set can be found in Deegan et al. (2012).

The results of this multi-disciplinary effort are synthesised in this chapter and provide insights into (1) the structural development of the NERZ, (2) the magmas feeding the NERZ plumbing system, and (3) the underlying mantle sources to the NERZ. This research approach thus provides a perspective from source processes to surface expression for oceanic rifts.

5.3 Field Occurrence and Petrography of the Dykes

The dykes exhibit a large degree of variability in terms of their field occurrence, even on the scale of a single intrusion. Thickness, orientation, and texture are frequently found to change, related to, e.g., changes in the competence of the host lithology (cf. Gudmundsson 2002) as can be seen
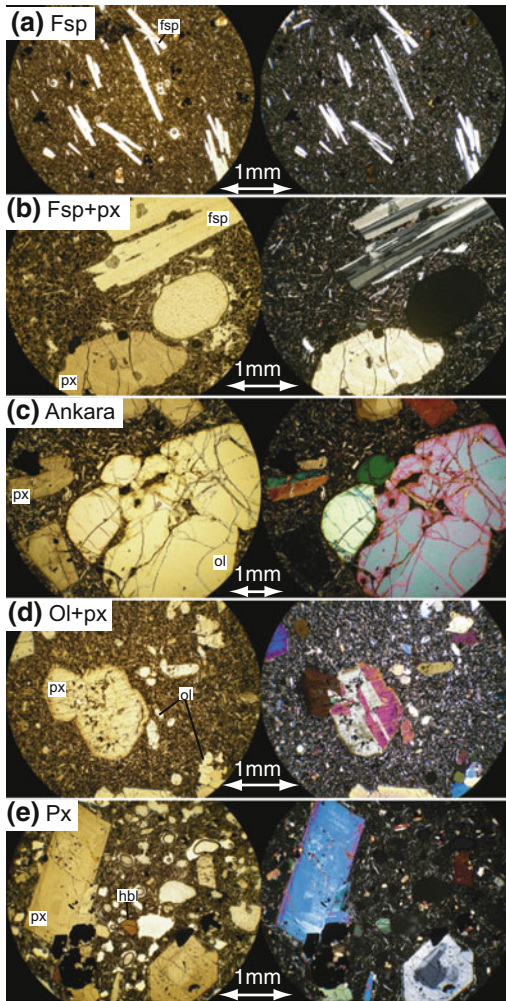
Fig. 5.4 Representative photomicrographs of the petrographic dyke groups (aphyric types not shown). **a** Feldspar-phyric group, **b** Feldspar and pyroxene-phyric group, **c** Ankaramite group, **d** Olivine and pyroxene-phyric group, and **e** Pyroxene-phyric group. Plane polarized view is shown on the left and cross polarized view on the right. Abbreviations: *Fsp* = feldspar, *px* = pyroxene, *ol* = olivine, *ankara* = ankaramite, *hbl* = hornblende. Figure modified from Delcamp et al. (2012)

rock (cf. Mathieu et al. 2008; Delcamp et al. 2012).

The mineralogy and petrography of the dykes, established both in the field, based on hand specimen scale observations, and using thin section microscopy (Fig. 5.4; Deegan et al. 2012; Delcamp et al. 2012) revealed recurring textures and the mineralogy of the dykes was used to characterise several petrographic groups:

1. *Aphyric group*. For the most part phenocryst free or only weakly-phyric. Occasional small crystals (<1 mm) of pyroxene and feldspar are observed in a micro- to cryptocrystalline, sometimes glassy, groundmass. Microphenocrysts generally constitute less than 5 % of the rock volume.

2. *Feldspar-rich group* ("fsp" dykes, Fig. 5.4a). Feldspar is the dominant phenocryst phase, occupying up to 50 % of the rock volume. Rare clinopyroxene, olivine, and Fe–Ti oxide crystals may be present with each constituting less than 10 % of the rock volume.

3. *Feldspar- and pyroxene-rich group* ("fsp + px" dykes, Fig. 5.4b). Feldspar and pyroxene are the main phenocryst phases, occupying up to 50 % of the rock volume, with feldspar generally more abundant than pyroxene. Minor olivine and Fe–Ti oxides may be present at up to 10 % of the rock volume.

4. *Ankaramite group* ("ankara", Fig. 5.4c). Olivine and pyroxene phenocrysts (up to 2 cm across) occupying between 40 and 60 % of the rock volume. Minor phenocryst phases also include amphibole and Fe–Ti oxides. Ankaramite groundmass ranges from cryptocrystalline to Fe–Ti oxide-rich.

5. *Olivine- and pyroxene-rich group* ("ol + px" dykes, Fig. 5.4d). Composed of a similar mineral assemblage to the ankaramite group, but with crystal contents ranging from 5 to 35 % of the rock volume. Phenocrysts are a few mm in size, making them substantially smaller than those in the ankaramites. The groundmass is generally rich in plagioclase and Fe–Ti oxides.

6. *Pyroxene-rich group* ("px" dykes, Fig. 5.4e). Clinopyroxenes are the major phenocryst forming phase occupying between 5 and 30 %
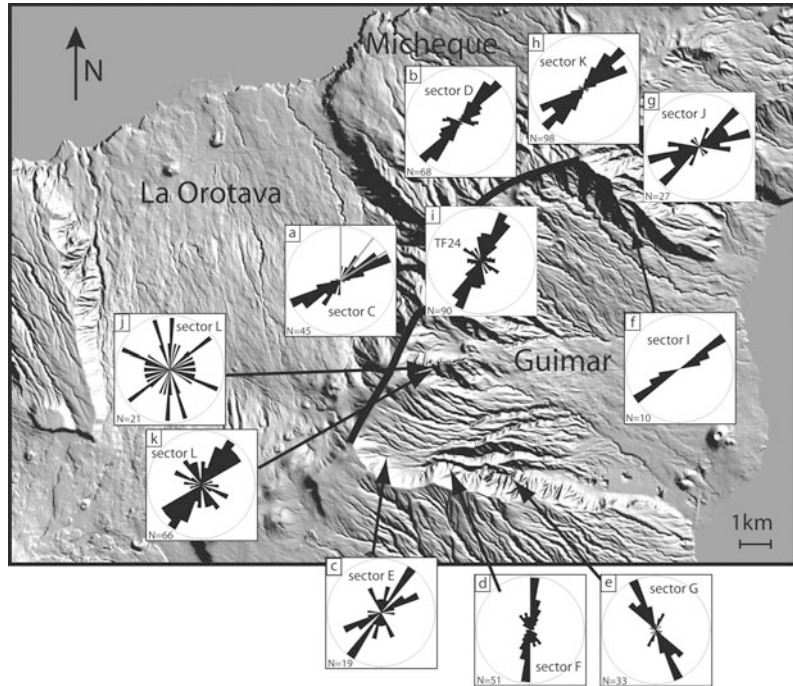
in Fig. 5.3. In particular, where there are two host lithologies in contact, the intruding dyke undergoes a structural change at the contact point (Fig. 5.3). Other notable variations on the intrusion scale include occasionally observed vesicular and brecciated dyke interiors, locally concentrated flow lobes, folding, and small-scale intrusive "fingers" into non-cohesive country

Fig. 5.5 *Rose* diagrams showing a large range of dyke orientations observed in the various portions of the NERZ. Note that dyke orientation along the rift is for most intrusions non-parallel to the rift axis. See text for details

of the rock volume. Minor phenocryst phases in this group include amphibole and Fe–Ti oxides at usually less than 10 % of the rock volume.

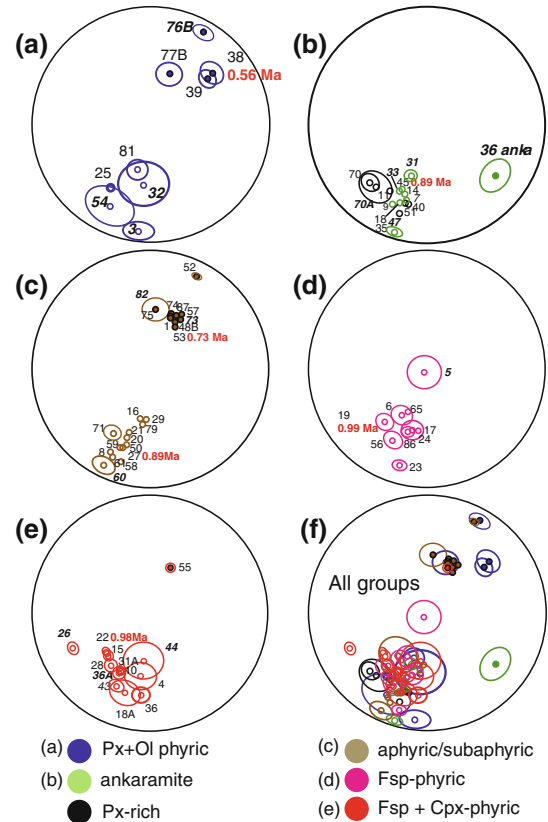## 5.4 Structural Evolution of the NERZ

Extensive field work has helped to gain insight into the structural development and organisation of the NERZ, in particular the link between dynamic rift-zone development and giant collapse events. In this context, several models have previously been discussed to explain rift zone organisation, as outlined in Chap. 4. The major finding arising from the field study presented in Delcamp et al. (2012) is that dyke orientation in the NERZ is not simply parallel to the rift axis or the collapse embayments but is frequently oblique to the walls of the main collapse scars (Fig. 5.5). This contrasts most previous observations from nature and experiments that document dykes parallel to the rift axis and the walls of collapse scars (e.g., Acocella and Neri 2009). The oblique dyke geometry of the NERZ is interpreted as being caused by flank

spreading and associated creep during successive pulses of emplacement of dykes and other shallow intrusions. Flank spreading would initially stabilise a rift, but after a critical amount of magma supply a collapse event would be triggered by continued intrusive activity. A small, but detectable change in dyke orientation on the rift axis seems to be also associated with the major landslides, implying that rift zones do indeed change dynamics and orientation due to external forces such as gravity-driven flank collapses (cf. Walter and Troll 2003; Walter et al. 2005; Carracedo and Troll, this volume). This result serves to change our perception of Ocean Island rifts from simple parallel alignments of intrusions to a complex and dynamic feeder system that develops in response to internal as well as external influences.

5.5 Magnetic Studies and Ages of the Dykes

Paleomagnetic studies of the NERZ were carried out by Carracedo et al. (2011) and Delcamp et al. (2010) to add temporal constraints to the

Fig. 5.6 Equal area
projection of mean
paleomagnetic results for
each site (Delcamp et al.
2010). Normal polarities
are indicated with open
symbols. Confidence
ellipses are shown for
some samples while others
are excluded for clarity.
Individual petrographic
groups are represented in
plots **a** to **e**. and all groups
are shown together in plot.
f Dykes dated by the
^{40}Ar/^{39}Ar method are
labelled with their age in
Ma (see Fig. 5.7 for more
detail). Note that
petrographic groups do not
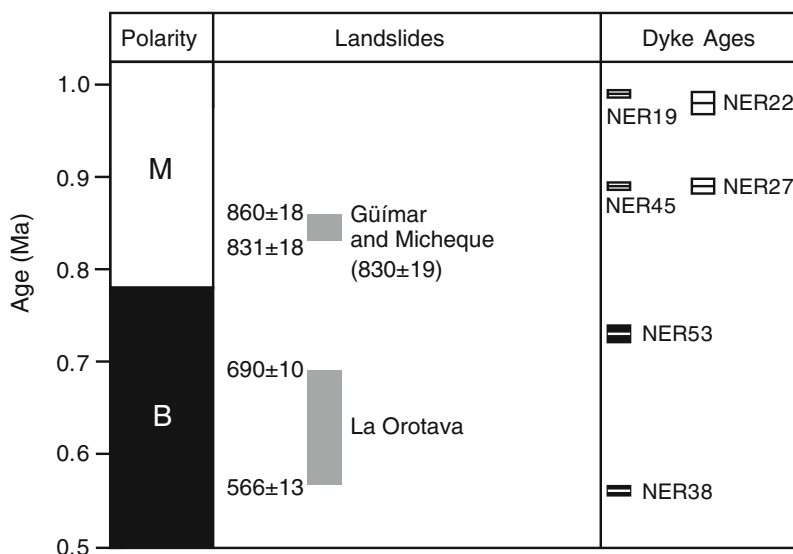correspond to individual
orientation trends

evolutionary history of the rift. The NERZ
shows a range in magnetic polarities, with the
dykes spanning at least two polarity intervals,
i.e., the Matuyama (reverse) and Bruhnes (nor-
mal) chrons (Figs. 5.6 and 5.7). The paleomag-
netic data hence points to the NERZ as being a
relatively long-lived system with, at times, a
considerable magma supply.

New ^{40}Ar/^{39}Ar ages reported in Carracedo
et al. (2011) and Delcamp et al. (2010) show that
intrusive activity on the NERZ is characterised
by a semi-continuous magma supply but with
swarms of dykes of various petrographic types
being intruded close in time, i.e., in pulses.
A peak in magma supply during the mid-
Pleistocene is thought to have led to flank
deformation and the subsequent collapses of the
Micheque, Güímar, and La Orotava edifices
(Carracedo et al. 2011). The paleomagnetic data
also record a 26° clockwise vertical-axis rotation
of the sampled rift core. Delcamp et al. (2010)

interpret this as a result of a local volcano-tec-
tonic response to strike-slip movements that
occurred successively on either side of the rift
axis due to flank instabilities. Central areas on
the rift may thus experience near surface rota-
tion—a feature also reported from other Canary
Islands, such as El Hierro (e.g., Széréméta et al.
1999). It is noteworthy that the petrographic
groupings of dykes do not correspond to specific
polarities nor are they spatially segregated
(Fig. 5.6), which suggests that the various pet-
rographic groups of dykes were not intruded in
distinct packages, but instead semi-simulta-
neously over the lifetime of the rift. A scenario
involving a number of smaller storage and fee-
der reservoirs is hence likely to have fed the
near-surface dyke intrusions, causing distinct
petrographic types to occur along the rift system
at the same time. The NERZ thus represents a
highly dynamic and changeable geological and
geo-morphological environment. Volcanic rift

Fig. 5.7 A comparison of the polarity scale (*left*, M = Matuyama, B = Brunhes), the timing of major collapse events on the NERZ (*centre*, Carracedo et al. 2011), and representative NERZ dyke ages (*right*) after Delcamp et al. (2010). Representative dyke ages are shown as rectangles whose vertical extent corresponds to the analytical uncertainty

zones such as the NERZ on Tenerife are thus not static structural features. In fact, they are characterised by concentrated pulses of active growth and giant destructions that result in measurable geometric re-arrangements.

5.6   Petrogenesis of the NERZ Magmas

The full geochemical and isotope data available for the dykes of the NERZ is reported in Deegan et al. (2012), with an overview provided here. The NERZ dykes can be classified as alkali magmas, similar to the other magma suites on Tenerife, such as the Teide-Pico Viejo complex (Fig. 5.8). Although the dykes of the NERZ display wide petrographic variability, most classify as basanites based on their major element composition (Fig. 5.8). The exceptions are crystal-rich ankaramite dykes, which plot as extremely mafic magma types due to their high content by volume of Mg-rich olivine and pyroxene (cf. Longpré et al. 2009).

Major element variation diagrams for the complete dyke suite display linear trends that are characteristic of fractional crystallisation of a mineral assemblage including olivine, clinopyroxene, plagioclase, Fe–Ti oxides, and apatite (Fig. 5.9). Magnetite has previously been identified as the

major Fe–Ti oxide phase in the dykes using reflected light microscopy (Fig. 5.9; Delcamp et al. 2010), which explains the kink in TiO_2 with increasing degrees of differentiation as magnetite fractionates. Trace element variations in the dykes are also broadly consistent with fractional crystallisation. Decreasing Sc, Ni, and Co with decreasing MgO reflects crystallisation of olivine and pyroxene (see Deegan et al. 2012; Fig. 5.9e, f). Fractional crystallisation was quantified by applying least squares minimisation to the aphyric samples, which most closely represent liquid compositions. The broad trends in the major element data can be readily explained by removal of plagioclase, clinopyroxene, Fe–Ti oxides, olivine, and apatite in the proportions 41:25:18:11:5, respectively (Fig. 5.9).

While the major and trace element variability in the dykes is largely controlled by fractional crystallisation, the isotope data suggest additional magmatic processes to have taken place. One key process which could account for the isotope variations in the dykes is crustal contamination of some of the rift zone magmas by hydrothermally altered components of the island edifice and/or oceanic sediments (Fig. 5.10).

Crustal contamination of Ocean Island magmas has traditionally been thought of as minimal. This is due to the relatively thin underlying oceanic crust and the assumption that magma injected into basaltic crust would be of similar
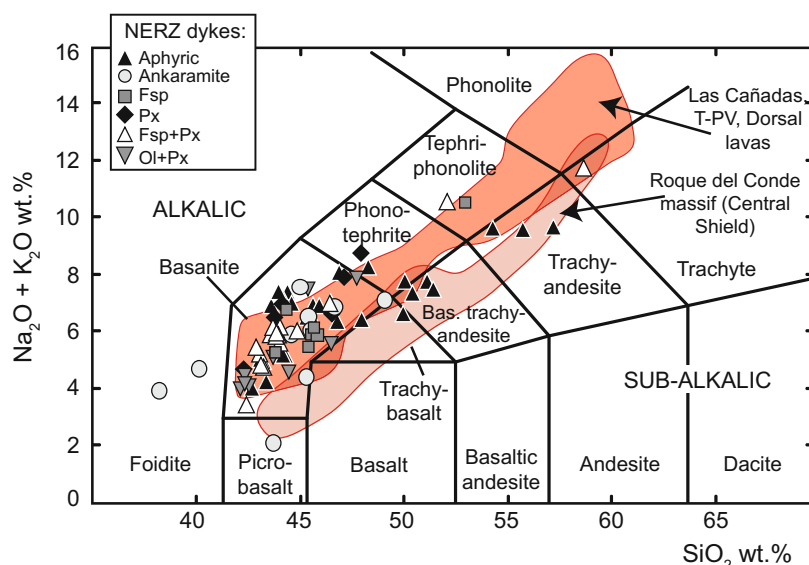
Fig. 5.8 Total alkali versus silica (*TAS*) plot for dykes of the Northeast rift zone (*NERZ*) with boundaries drawn after Irvine and Baragar (1971) and nomenclature after Le Maitre et al. (1989). Symbols correspond to the petrographic groupings of the NERZ. Shaded fields are drawn usi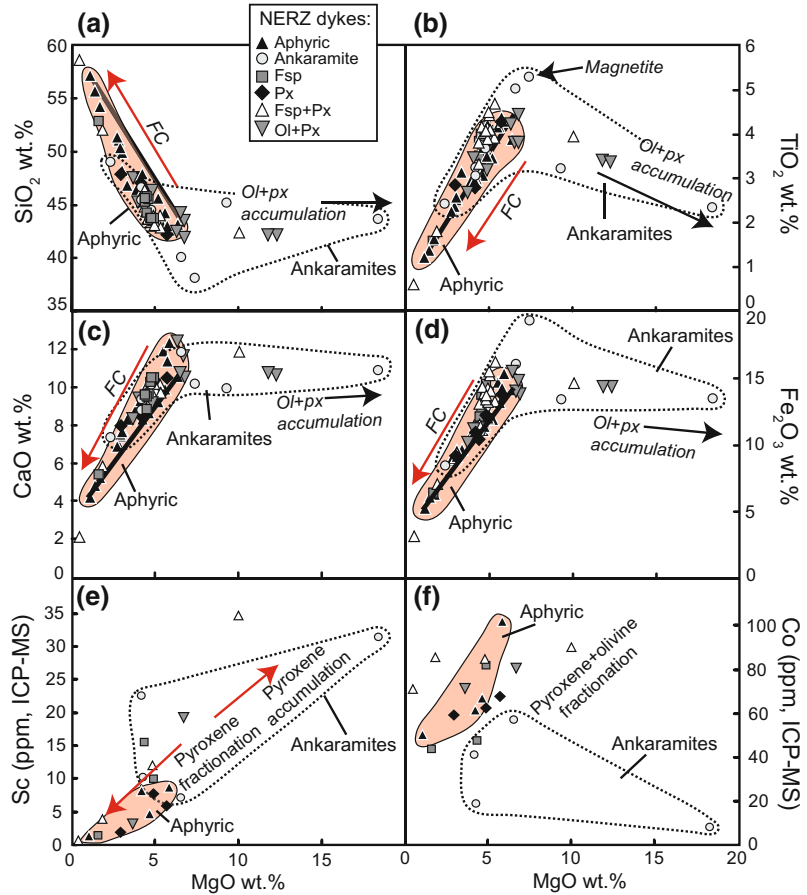ng data for the Central Shield (Roque del Conde) after Thirlwall et al. (2000) and for the Las Cañadas volcano, the Teide-Pico Viejo complex (T-PV), and lavas from the NERZ after Ablay et al. (1998) and Neumann et al. (1999). Figure modified after Deegan et al. (2012)

enough composition so that contamination would in effect be absent. However, in practice, crustal contamination by various components of the ocean crust, overlying sediments, and the island edifice itself is becoming increasingly recognized in Ocean Island settings (e.g., Clague et al. 1995; Bohrson and Reid 1997; Garcia et al. 1998; Kent et al. 1999; Harris et al. 2000; Wolff et al. 2000; Gurenko et al. 2001; Troll and Schmincke 2002; Hansteen and Troll 2003; Gaffney et al. 2005; Legendre et al. 2005; Wiesmaier 2010). On Tenerife, the most likely contaminants are the plutonic rocks of the island core and variably altered shallow felsic materials, which display a large compositional diversity (e.g., Palacz and Wolff 1989; Wolff et al. 2000; Wiesmaier et al. 2012).

Oxygen isotope analysis of the dykes of the NERZ indicates that some dyke intrusions bear witness to low temperature alteration, i.e., those with coupled high $\delta^{18}O$ and H_2O wt. % values (Deegan et al. 2012). A number of dykes with regular H_2O values still show $\delta^{18}O$ values that are elevated relative to the mantle range, which cannot be readily explained by closed-system fractional crystallisation or post-eruptive alteration (see the Rayleigh fractionation curve on Fig. 5.10; and also Sheppard and Harris 1985). Mixing models suggest that some of the variability in the NERZ data may be explained by uptake of ^{18}O from a combination of oceanic sediment and hydrothermally altered material from the island edifice (Fig. 5.10). Similarly, minor variation in $^{87}Sr/^{86}Sr$ and $^{143}Nd/^{144}Nd$ values, that trend away from the upper mantle range and towards more crustal values, can be explained by minor interaction between some batches of NERZ magma with hydrothermally altered island edifice material (Fig. 5.11; Deegan et al. 2012). This is plausible, given that assimilation of such hydrothermally altered felsic material has been recognized previously for Tenerife (e.g., Palacz and Wolff 1989; Wolff et al. 2000; Wiesmaier 2010). Altered felsic rocks probably occupy a substantial portion of the subvolcanic pile in which the NERZ magmas resided and into which the NERZ dykes were intruded and would hence have been readily available for

Fig. 5.9 Major and trace element variation diagrams for dykes of the NERZ. Aphyric samples are shown as *black triangles* and, being largely phenocryst-free, are representative of true liquid compositions. *Solid black lines* are fractional crystallisation trajectories for a model involving crystallisation of plagioclase, clinopyroxene, Fe–Ti oxides, olivine, and apatite in the proportions 41:25:18:11:5, respectively (see text). FC = fractional crystallisation. Figure modified after Deegan et al. (2012)

interaction. Note that assimilation of ocean sediments and/or hydrothermally altered ocean crust and island edifice has been discussed in the context of several of the Canary Islands, not only Tenerife (e.g., Marcantonio et al. 1995; Thirwall et al. 1997; Gurenko et al. 2001; Troll and Schmincke 2002; Hansteen and Troll 2003; Aparicio et al. 2006, 2010; Troll et al. 2012). The effects of these late stage processes need to therefore be accounted for before attempting to define the mantle processes giving rise to the primary magmas of the NERZ.

Concerning magma generation beneath the NERZ, the Pb isotope data presented in Deegan et al. (2012) provide insights into the nature of the mantle source and, in combination with magnetic polarity data (Delcamp et al. 2010), the genetic ties between various stages in island growth. Lead isotopes are not expected to be overly sensitive to

contamination by hydrothermally altered island edifice since Pb does not appear to undergo isotopic exchange during alteration (Cousens et al. 1993; Gaffney et al. 2005) and hence they are particularly useful for the NERZ. Most of the Pb isotope data for the NERZ plot below but roughly parallel to the Northern Hemisphere Reference Line (NHRL, Hart 1984) which represents a mixture between depleted upper mantle (DMM) and a mantle that involves an ancient subducted component (HIMU) (Fig. 5.12). In this context, the NERZ Pb isotope data are consistent with derivation from a young HIMU source, in which the subducted ocean crust component has resided less than 1.5 Ga in the source region (Thirlwall 1997; Geldmacher and Hoernle 2000, 2001; Simonsen et al. 2000; Gurenko et al. 2009). Two of the dykes plot above the NHRL on Fig. 5.12, which, in combination with their elevated $\delta^{18}O$
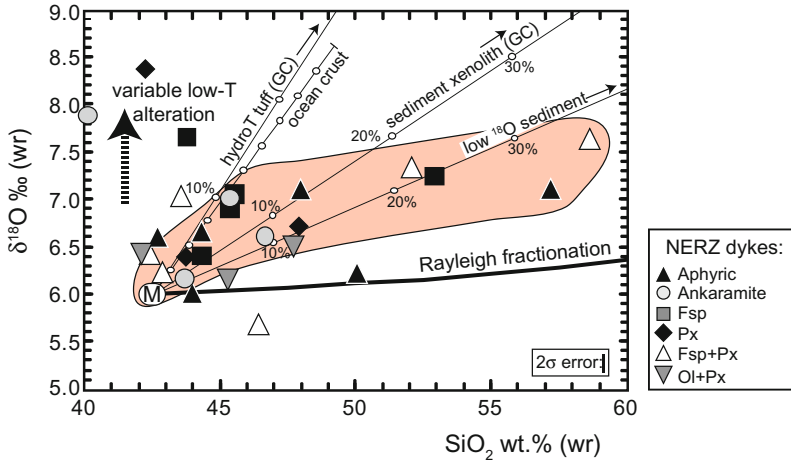
Fig. 5.10 A $\delta^{18}O$ versus SiO_2 plot for dykes of the NERZ. Most of the dykes exhibit large and variable deviation from the trend expected for a magmatic suite related by closed system fractional crystallisation (Rayleigh fractionation from a mantle parent, "M"). Mixing models are shown to illustrate that some of the $\delta^{18}O$ variability in the dykes can be explained by mixing between a parental mantle source and hydrothermally altered edifice rock and/or ocean sediment. A mixing line is also shown for ocean crust (layer 2 from Hansteen and Troll 2003). Symbols on the *mixing lines* are 10 % mixing increments. The *orange shaded* field serves to highlight the main magmatic contamination trend among the dykes. Figure modified after Deegan et al. (2012)
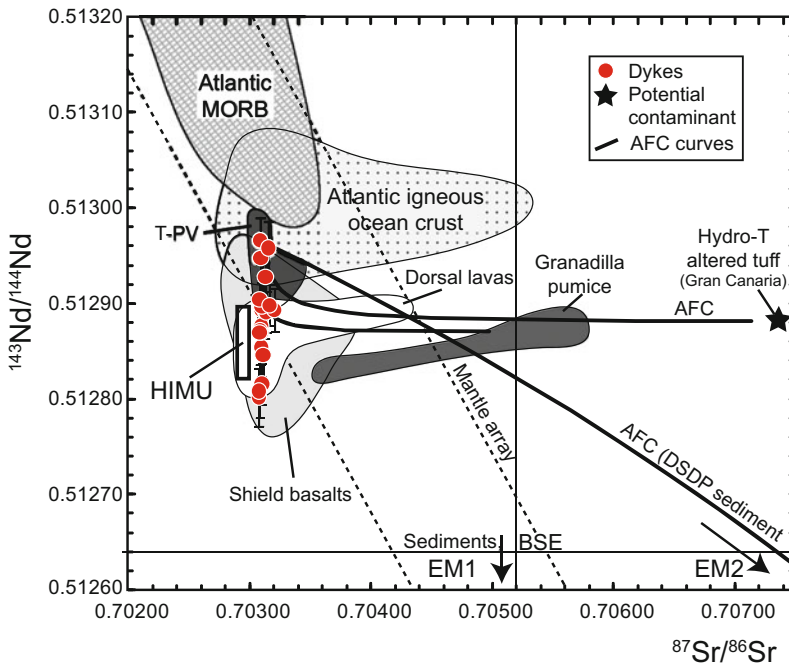

Fig. 5.11 $^{87}Sr/^{86}Sr$—$^{143}Nd/^{144}Nd$ isotope variation diagram for dykes of the NERZ, and some reference fields including: Atlantic MORB (Ito et al. 1987); Atlantic igneous ocean crust (Hoernle 1998); Tenerife shield basalts (Simonsen et al. 2000; Gurenko et al. 2006); the Teide-Pico Viejo (T-PV) complex (Wiesmaier et al. 2010); NERZ lavas (Simonsen et al. 2000); and the Granadilla pumice (Palacz and Wolff 1989). A hydrothermally altered tuff from Gran Canaria is also plotted (Troll 2001). The dykes of the NERZ form a roughly linear array between the fields for HIMU-type mantle and Atlantic MORB. A number of dykes are slightly offset from the array. Their offset can be explained by incorporation of small amounts of hydrothermally altered material during magma storage in the island edifice (heavy black lines are assimilation-fractional crystallisation (AFC) curves)
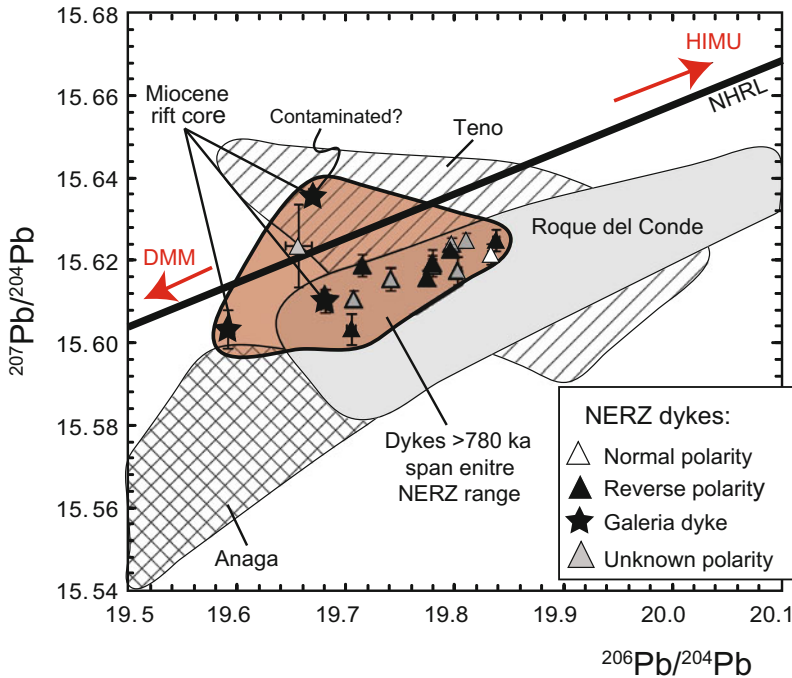
Fig. 5.12 $^{206}Pb/^{204}Pb$—$^{207}Pb/^{204}Pb$ isotope variation diagram for dykes of the NERZ, with symbols corresponding to the ages of the dykes. Magnetic polarities are taken from Delcamp et al. (2010): reverse polarity dykes are ≥780 ka old; normal polarity dyke is ≤780 ka old. *Black stars* are *galería* samples taken from the core of the rift and hence represent an older, likely Pliocene, part of the system (Carracedo et al. 2011)
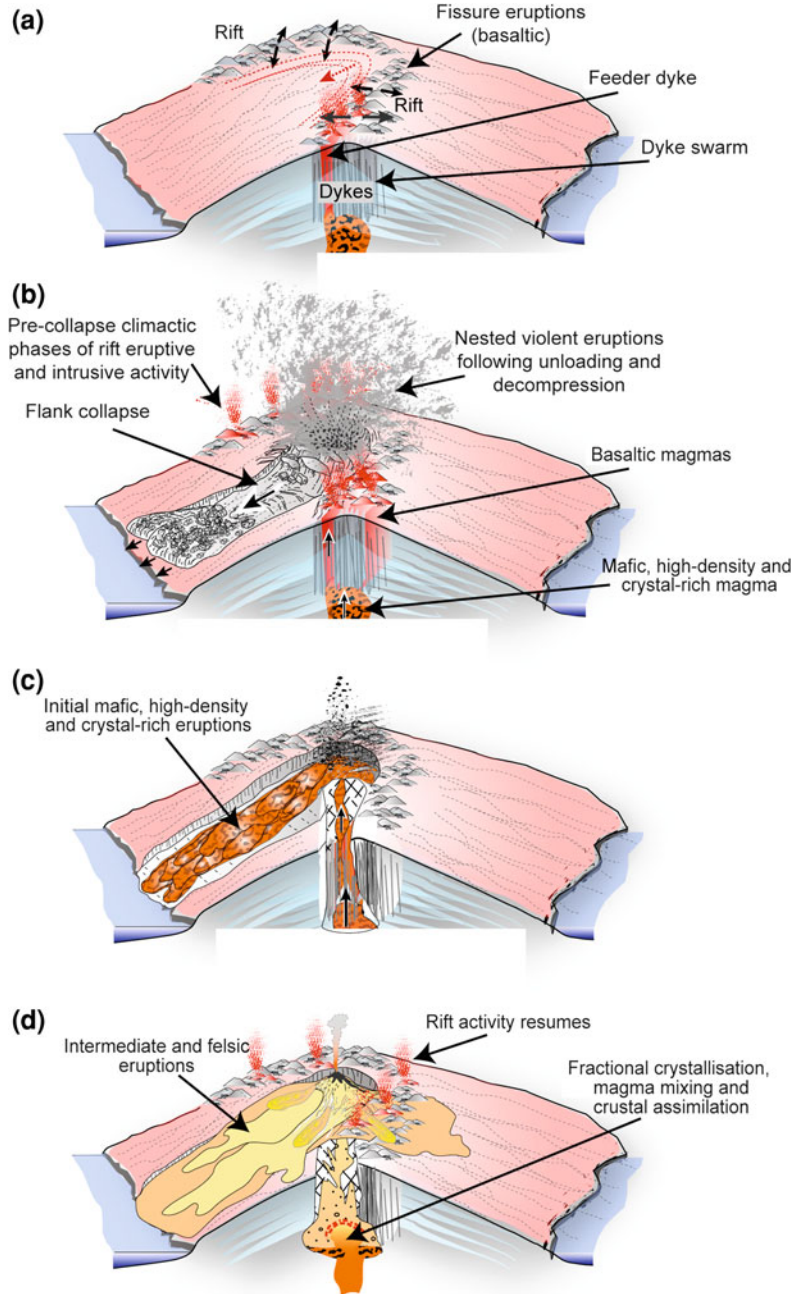
values, points to more intense sediment contamination of these two samples. Discarding samples that show evidence for crustal contamination, Strontium-Neodymium isotopes are consistent with DMM + HIMU mantle mixing (Deegan et al. 2012).

Using magnetic polarity data obtained for some of the dykes (Delcamp et al. 2010), we can place temporal constraints on the isotope data. As can be seen in Fig. 5.12, the Pb isotope compositional range of the NERZ has been largely unchanged through most of its evolution, i.e., the old *galería* dykes and the dykes of normal, reverse, and unknown polarities span the entire NERZ range, and do not form isotopically distinguishable groups. This observation suggests that the mantle source feeding the NERZ has been isotopically constant through its lifetime. Moreover, of the three shield-stage volcanoes on Tenerife (Teno, Anaga, and Roque del Conde), the NERZ is isotopically most

similar to the old central edifice of Roque del Conde (Fig. 5.12). It therefore appears likely that the NERZ had a different "mantle highway" than both Teno and Anaga, and instead formed as an extension of the Central Shield, gradually growing toward what is now Anaga in the NE (Fig. 5.1, see also Guillou et al. 2004; Carracedo et al. 2011).

The Pb-isotope signature of the NERZ is also similar to the Las Cañadas volcano (Simonsen et al. 2000) suggesting that they both shared a similar parental source too. This is not surprising as the Pleistocene NERZ was emplaced and erupted coeval to the central Las Cañadas volcano (e.g., Ancochea et al. 1990; Bryan et al. 1998; Edgar et al. 2002; Carracedo et al. 2011). The relatively young Teide-Pico Viejo (T-PV) complex, however, extends towards less radiogenic $^{206}Pb/^{204}Pb$—$^{207}Pb/^{204}Pb$ values, which, coupled with high $^{143}Nd/^{144}Nd$ values, suggests that this most recent phase of magmatism on Tenerife had

Fig. 5.13 Schematic model of Canary Island rift evolution (after Carracedo et al. 2011). Note that the rift evolution proceeds until high intrusive activity causes flank collapses to occur. Following such a catastrophic collapse, the plumbing system needs to readjust, leading to structural and petrologic modifications of the rift (cf. Longpré et al. 2009; Manconi et al. 2009; Delcamp et al. 2010, 2012; Carracedo et al. 2011)

a slightly different mantle source with a greater input of DMM material (i.e., a lower proportion of a deep HIMU-plume component).

The persistence of a HIMU-dominated mantle source throughout the lifetime of the NERZ can be interpreted in the context of the "blob" model for the Canary Islands (Hoernle et al. 1991;

Hoernle and Schmincke 1993). This model involves formation of a zone of discrete HIMU mantle blobs at the top of a mantle plume beneath the Canaries. These blobs become entrained with upper asthenospheric mantle (DMM), giving rise to the mixed DMM + HIMU mantle isotope signal of the Canaries. We suggest that a large

column of HIMU-type mantle, or a quick succession of compositionally similar HIMU-blobs, occupied the melting zone beneath central Tenerife from the Miocene to Pleistocene. This was possibly accommodated for such a long period of time by slow plate movement beneath the Canaries ($\sim$ 10 mm yr^{-1}; Hoernle and Schmincke 1993 and references therein). The recent T-PV complex appears to reflect a lesser influence of the HIMU blob and greater incorporation of DMM material, possibly due to an increase of edge-DMM entrainment into the melting zone and thinning of the blob(s) with time (see Deegan et al. 2012).

5.7   Unravelling the NERZ from Source to Surface

The recent intense and multi-disciplinary research efforts to unravel the structural and petrogenetic history of the NERZ underscores the premise that ocean island rift zones are long-lived, complex, and dynamically evolving systems. They can neither be thought of as a simple parallel arrangement of dykes and volcanic vents along fractures, nor as purely reflecting long-lived ocean crust fractures. Indeed, it has been shown that the NERZ is a dynamic morphological environment, which developed from a series of intrusive pulses interspersed with periods of relative quiescence, but also with flank creep, and particularly with collapse events that changed the structural arrangement of dyke intrusions and eruptive sites repeatedly (e.g., Delcamp et al. 2010, 2012; Carracedo et al. 2011; and Carracedo and Troll, this volume; see also Fig. 5.13 for a summary).

In terms of petrogenesis, the history of the NERZ began with magma generation from a long-lived HIMU-dominated mantle source. Following segregation from the mantle region, many of the NERZ magmas underwent fractional crystallisation, and some underwent assimilation of ocean sediments and hydrothermally altered island edifice material. Isotope geochemistry places the initiation and growth of the NERZ into the wider geological context of

Tenerife. The data discussed in this chapter, in conjunction with geochronological evidence (Carracedo et al. 2011), support a model of the NERZ magmas being related to the magma source of the central edifice (Roque del Conde and Las Cañadas volcanoes), which implies that the NERZ likely originated from the central part of Tenerife to eventually link up with the Anaga edifice in the NE.

References

Ablay GJ, Carroll MR, Palmer MR, Martí J, Sparks RSJ (1998) Basanite-phonolite lineages of the teide-pico viejo volcanic complex, tenerife, Canary Islands. J Petrol 39:905–936

Abratis M, Schmincke H-U, Hansteen TH (2002) Composition and evolution of submarine volcanic rocks from the central and western Canary Islands. Int J Earth Sci 91:562–582

Acocella V, Neri M (2009) Dike propagation in volcanic edifices: overview and possible developments. Tectonophysics 471:67–77

Ancochea E, Fuster JE, Ibarrola E, Cendrero A, Coello J, Hernan F, Cantagrel JM, Jamond C (1990) Volcanic evolution of the island of tenerife (Canary Islands) in the light of new K-Ar data. J Volcanol Geotherm Res 44:231–249

Aparicio A, Bustillo MA, Garcia R, Araña V (2006) Metasedimentary xenoliths in the lavas of the timanfaya eruption (1730–1736, Lanzarote, Canary Islands): metamorphism and contamination processes. Geol Mag 143:181–193

Aparicio A, Tassinari CCG, García R, Araña V (2010) Sr and Nd isotope composition of the metamorphic, sedimentary and ultramafic xenoliths of lanzarote (Canary Islands): implications for magma sources. J Volcanol Geotherm Res 189:143–150

Bohrson WA, Reid MR (1997) Genesis of silicic peralkaline volcanic rocks in an ocean island setting by crustal melting and open system processes: Socorro Island, Mexico. J Petrol 38:1137–1166

Bryan SE, Martí J, Cas RAF (1998) Stratigraphy of the bandas del sur formation: an extracaldera record of quaternary phonolitic explosive eruptions from the las cañadas edifice, tenerife (Canary Islands). Geol Mag 135:605–636

Carracedo JC (1975) Estudio Paleomagnético de la Isla de Tenerife. Dissertation, Universidad Complutense de Madrid

Carracedo JC (1979) Paleomagnetismo e Historia Volcánica de Tenerife: Tenerife, Aula de Cultura del Cabildo de Tenerife, p 81

Carracedo JC (1994) The Canary Islands: an example of structural control on the growth of large oceanic island volcanoes. J Volcanol Geotherm Res 60:225–242

Carracedo JC (1996) Morphological and structural evolution of the western Canary Islands: hotspot induced three-armed rifts or regional tectonic trends? J Volcanol Geotherm Res 72:151–162

Carracedo JC (1999) Growth, structure, instability and collapse of Canarian volcanoes and comparisons with Hawaiian volcanoes. J Volcanol Geotherm Res 94:1–19

Carracedo JC, Rodríguez Badiola E, Soler V (1992) The 1730–1736 eruption of Lanzarote: an unusually long, high-magnitude fissural basaltic eruption in the recent volcanism of the Canary Islands. J Volcanol Geotherm Res 53:239–250

Carracedo JC, Day S, Guillou H, Rodríguez Badiola E, Canas JA, Pérez Torrado FJ (1998) Hotspot volcanism close to a passive continental margin: the Canary Islands. Geol Mag 135:591–604

Carracedo JC, Rodríguez Badiola E, Guillou H, De La Nuez J, Pérez Torrado FJ (2001) Geology and volcanology of La Palma and El Hierro, Western Canaries. Estud Geol 57:175–273

Carracedo JC, Rodríguez Badiola E, Guillou H, Paterne M, Scaillet S, Pérez Torrado FJ, Paris R, Criado C, Hansen A, Arnay M, González Reimers E, Fra-Paleo U, González Pérez R (2006) Los volcanes del Parque Nacional del Teide: El Teide, Pico Viejo y las dorsales activas de Tenerife. In: Carracedo JC (ed) Los Volcanes del Parque Nacional del Teide, Serie Técnica: Madrid, Organismo de Parques Nacionales, Ministerio del Medio Ambiente, Madrid, pp 175-199

Carracedo JC, Rodríguez Badiola E, Guillou H, Paterne M, Scaillet S, Pérez Torrado FJ, Paris R, Fra-Paleo U, Hansen A (2007) Eruptive and structural history of Teide volcano and rift zones of Tenerife, Canary Islands. Geol Soc Am Bull 19:1027–1051

Carracedo JC, Guillou H, Nomade S, Rodríguez Badiola E, Paris R, Troll VR, Wiesmaier S, Delcamp A, Fernández-Turiel JL (2011) Evolution of ocean-island rifts: The northeast rift zone of Tenerife, Canary Islands. Geol Soc Am Bull 123:562–584

Carracedo JC, Troll VR (2012) Structural and geological elements of the Teide Volcanic complex: rift zones and gravitational collapses (this volume)

Clague DA, Moore JG, Dixon JE, Friesen WB (1995) Petrology of submarine lavas from Kilauea's Puna Ridge. Hawaii. J Petrol 36:299–349

Cousens BL, Spera FJ, Dobson PF (1993) Post-eruptive alteration of silicic ignimbrites and lavas, Gran Canaria, Canary Islands: strontium, neodymium, lead, and oxygen isotopic evidence. Geochim Cosmochim Acta 57:631–640

Deegan FM, Troll VR, Barker AK, Chadwick JP, Harris C, Delcamp A, Carracedo JC (2012) Crustal versus source processes recorded in dykes of the Northeast volcanic rift zone of Tenerife, Canary Islands. Chem Geol 334:324–344

Delcamp A, Petronis MS, Troll VR, Carracedo JC, van Wyk de Vries B, Perez-Torrado FJ (2010) Vertical axis rotation of the upper portions of the north-east rift of Tenerife Island inferred from paleomagnetic data. Tectonophysics 492:40–59

Delcamp A, Troll VR, van Wyk de Vries B, Carracedo JC, Petronis MS, Pérez-Torrado FJ, Deegan FM (2012) Stabilisation and destabilization of ocean island rift-zones: the NE-rift of Tenerife, Canary Islands. Bull Volcanol 74:963–980

Dieterich JH (1988) Growth and persistence of Hawaiian volcanic rift zones. J Geophys Res 93:4258–4270

Edgar CJ, Wolff JA, Nichols HJ, Cas RAF, Martí J (2002) A complex Quaternary ignimbrite-forming phonolitic eruption: the Poris member of the Diego Hernández Formation (Tenerife, Canary Islands). J Volcanol Geotherm Res 118:99–130

Fagereng A, Harris C, LaGrange M, Stevens G (2008) Stable isotope study of the Archean rocks of the Vredefort impact structure, central Kaapvaal Craton, South Africa. Contrib Mineral Petrol 155:63–78

Fiske R, Jackson ED (1972) Orientation and growth of Hawaiian volcanic rifts: the effect of regional structure and gravitational stresses. Proc R Soc London 329:299–326

Gaffney AM, Nelson BK, Reisberg L, Eiler J (2005) Oxygen-osmium isotope systematics of West Maui lavas: a record of shallow-level magmatic processes. Earth Planet Sci Lett 239:122–139

Garcia MO, Ito E, Eiler JM, Pietruszka AJ (1998) Crustal contamination of Kilauea volcano magmas revealed by oxygen isotope analyses of glass and olivine from Puu Oo eruption lavas. J Petrol 39:803–817

Geldmacher J, Hoernle K (2000) The 72 Ma geochemical evolution of the Madeira hotspot (eastern North Atlantic): recycling of Paleozoic ($\leq$500 Ma) oceanic lithosphere. Earth Planet Sci Lett 183:73–92

Geldmacher J, Hoernle K (2001) Corrigendum to: 'The 72 Ma geochemical evolution of the Madeira hotspot (eastern North Atlantic): recycling of Paleozoic ($\leq$ 500 Ma) oceanic lithosphere' (Earth Planet Sci Lett 2000 183:73–92). Earth Planet Sci Lett 186:333

Gudmundsson A (2002) Emplacement and arrest of sheets and dykes in central volcanoes. J Volcanol Geotherm Res 116:279–298

Guillou H, Carracedo JC, Pérez Torrado F, Rodríguez Badiola E (1996) K-Ar ages and magnetic stratigraphy of a hotspot-induced, fast grown oceanic island: El Hierro, Canary Islands. J Volcanol Geotherm Res 73:141–155

Guillou H, Carracedo JC, Paris R, Pérez Torrado FJ (2004) K/Ar ages and magnetic stratigraphy of the miocene-pliocene shield volcanoes of tenerife, canary islands: implications for the early evolution of tenerife and the canarian hotspot age progression. Earth Planet Sci Lett 222:599–614

Gurenko AA, Chaussidon M, Schmincke H-U (2001) Magma ascent and contamination beneath one intra-plate volcano: evidence from S and O isotopes in glass inclusions and their host clinopyroxenes from Miocene basaltic hyaloclastites southwest of Gran Canaria (Canary Islands). Geochimica et Cosmochimica Acta 65:4359–4374

Gurenko AA, Hoernle KA, Hauff F, Schmincke H-U, Han D, Miura YN, Kaneoka I (2006) Major, trace

element and Nd-Sr-Pb-O-He-Ar isotope signatures of shield stage lavas from the central and western Canary Islands: insights into mantle and crustal processes. Chem Geol 233:75–112

Gurenko AA, Sobolev AV, Hoernlae KA, Hauff F, Schmincke H-U (2009) Enriched, HIMU-type peridotite and depleted recycled pyroxenite in the canary plume: a mixed-up mantle. Earth Planet Sci Lett 277:514–524

Hansen A (2009) Volcanología y Geomorfología de la Etapa de Rejuvenecimiento Plio-Pleistocena de Gran Canaria (Islas Canarias) Ph.D. thesis, Las Palmas, Gran Canaria, University of Las Palmas

Hansteen TH, Troll VR (2003) Oxygen isotope composition of xenoliths from the oceanic crust and volcanic edifice beneath Gran Canaria (Canary Islands): consequences for crustal contamination of ascending magmas. Chem Geol 193:181–193

Harris C, Smith HS, le Roex AP (2000) Oxygen isotope composition of phenocrysts from Tristan da Cunha and Gough Island lavas: variation with fractional crystallization and evidence for assimilation. Contrib Mineral Petrol 138:164–175

Hart SR (1984) A large scale isotope anomaly in the southern hemisphere mantle. Nature 309:753–757

Hoernle K (1998) Geochemistry of Jurassic ocean crust beneath Gran Canaria (Canary Islands): implications for crustal recycling and assimilation. J Petrol 39:859–880

Hoernle K, Schmincke H-U (1993) The role of partial melting in the 15-Ma geochemical evolution of Gran Canaria: a blob model for the Canary hotspot. J Petrol 34:599–626

Hoernle K, Tilton G, Schmincke H-U (1991) Sr-Nd-Pb isotopic evolution of Gran Canaria: evidence for shallow enriched mantle beneath the Canary Islands. Earth Planet Sci Lett 106:44–63

Irvine TN, Baragar WRA (1971) A guide to the chemical classification of the common volcanic rocks. Can J Earth Sci 8:523–548

Ito E, White WM, Göpel C (1987) The O, Sr, Nd and Pb isotope geochemistry of MORB. Chem Geol 62:157–176

Kent AJR, Norman MD, Hutcheon ID, Stolper EM (1999) Assimilation of seawater-derived components in an oceanic volcano: evidence from matrix glasses and glass inclusions from Loihi Seamount, Hawaii. Chem Geol 156:299–319

Legendre C, Maury RC, Caroff M, Guillou H, Cotton J, Chauvel C, Bollinger C, Hémond C, Guille G, Blais S, Rossi P, Savanier D (2005) Origin of exceptionally abundant phonolites on Ua Pou Island (Marquesas, French Polynesia): Partial melting of basanites followed by crustal contamination. J Petrol 46:1925–1962

Le Maitre RW, Bateman P, Dudek A, Keller J, Lameyre J, Le Bas MJ, Sabine PA, Schmid R, Sorensen H, Streckeisen A, Woolley AR, Zanettin B (1989) A classification of igneous rocks and glossary of terms. Blackwell, Oxford

Longpré M-A, Troll VR, Walter TR, Hansteen TH (2009) Volcanic and geochemical evolution of the Teno massif, Tenerife, Canary Islands: some repercussions of giant landslides on ocean island magmatism. Geochem Geophys Geosy 10:Q12017. doi: 10.1029/2009GC002892

Manconi A, Longpré M-A, Walter TR, Troll VR, Hansteen TH (2009) The effects of flank collapses on volcano plumbing systems. Geology 37:1099–1102

Marcantonio F, Zindler A, Elliott T, Staudigel H (1995) Os isotope systematics of La Palma, Canary Islands: evidence for recycled crust in the mantle source of HIMU ocean islands. Earth Planet Sci Lett 133:197–410

Mathieu L, van Wyk de Vries B, Troll VR, Holohan EP (2008) Dykes, cups, saucers and sills: Analogue experiments on magma intrusion into brittle rocks. Earth Planet Sci Lett 271:1–13

Navarro JM, Farrujia I (1989) Plan Hidrológico Insular de Tenerife: Zonificación Hidrológica, Aspectos Geológicos e Hidrogeológicos: Cabildo Insular de Tenerife, Santa Cruz de Tenerife, p 133

Neumann E-R, Wulff-Pedersen E, Simonsen SL, Pearson NJ, Martí J, Mitjavila J (1999) Evidence for fractional crystallization of periodically refilled magma chambers in Tenerife, Canary Islands. J Petrol 40:1089–1123

Palacz ZA, Wolff JA (1989) Strontium, neodymium and lead isotope characteristics of the Granadilla Pumice, Tenerife: a study of the causes of strontium isotope disequilibrium in felsic pyroclastic deposits. In: Saunders AD, Norry MJ (eds) Magmatism in the ocean basins. Geol Soc Spec Publ 42: 147–159

Roeser HA (1982) Magnetic anomalies in the magnetic quiet zone off Morocco. In: Rad U, Hinz K, Sarnthein M, Seibold E (eds) Geology of the northwest african continental margin. Springer, Berlin, pp 61–68

Sheppard SMF, Harris C (1985) Hydrogen and oxygen isotope geochemistry of Ascension Island lavas and granites: variation with crystal fractionation and interaction with seawater. Contrib Mineral Petrol 91:74–81

Simonsen SL, Neumann E-R, Seim K (2000) Sr-Nd-Pb isotope and trace-element geochemistry evidence for a young HIMU source and assimilation at Tenerife (Canary Island). J Volcanol Geotherm Res 103:299–312

Swanson DA, Duffield WA, Fiske RS (1976) Displacements of the south flank of Kilauea Volcano: the result of forceful intrusions of magma into the rift zones. US Geol Surv Prof Paper 963:39

Széréméta N, Laj C, Guillou H, Kissel C, Mazaud A, Carracedo JC (1999) Geomagnetic paleosecular variation in the brunhes period, from the island of El Hierro (Canary Islands). Earth Planet Sci Lett 165:241–253

Thirlwall MF (1997) Pb isotopic evidence for OIB derivation from young HIMU mantle. Chem Geol 139:51–74

Thirlwall MF, Singer BS, Marriner GF (2000) ^{39}Ar-^{40}Ar ages and geochemistry of the basaltic shield stage of

Tenerife, Canary Islands, Spain. J Volcanol Geotherm Res 103:247–297

Troll VR (2001) Evolution of large peralkaline silicic magma chambers and associated caldera systems: a case study from Gran Canaria, Canary Islands. Ph. D. thesis Christian-Albrechts-Universität zu Kiel

Troll VR, Schmincke H-U (2002) Alkali-feldspar in compositionally zoned peralkaline rhyolite/trachyte ignimbrite "A", Gran Canaria: implications for magma mixing and crustal recycling. J Petrol 43:243–270

Troll VR, Klügel A, Longpré M-A, Burchardt S, Deegan FM, Carracedo JC, Wiesmaier S, Kueppers U, Dahren B, Blythe LS, Hansteen TH, Freda C, Budd DA, Jolis EM, Jonsson E, Meade FC, Berg SE, Mancini L, Polacci M, Pedroza K (2012) Floating stones off El Hierro, Canary Islands: xenoliths of pre-island sedimentary origin in the early products of the October 2011 eruption. Solid Earth 3:97–110

Vennemann TW, Smith HS (1990) The rate and temperature of reaction of ClF$_3$ with silicate minerals, and their relevance to oxygen isotope analysis. Chem Geol 86:83–88

Walker GPL (1986) Koolau dike complex, Oahu: Intensity and origin of a sheeted-dike complex high in a Hawaiian volcanic edifice. Geology 14:310–313

Walker GPL (1987) The dike complex of Koolau Volcano, Oahu: internal structure of a Hawaiian Rift Zone. In: Decker RW, Wright RL, Stauffer PJ (eds) Volcanism in Hawaii, vol 2. US Geol Surv Prof Pap 1350:961–993

Walker GPL (1992) Coherent intrusion complexes in large basaltic volcanoes; a new structural model. In: Harris PG, Cox KG, Baker PE (eds) Essays on magmas and other earth fluids, vol 50. Elsevier, The Netherland, pp 41–54

Walter TR, Schmincke H-U (2002) Rifting, recurrent landsliding and Miocene structural reorganization on NW-Tenerife (Canary Islands). Int J Earth Sci 91:615–628

Walter TR, Troll VR (2003) Experiments on rift zone evolution in unstable volcanic edifices. J Volcanol Geotherm Res 127:20–107

Walter TR, Troll VR, Cailleau B, Belousov A, Schmincke H-U, Amelung F, v.d.Bogaard P (2005) Rift zone reorganisation through flank instability in ocean island volcanoes: an example from Tenerife, Canary Islands. Bull Volcanol 67:281–291

Wiesmaier S (2010) Magmatic differentiation and bimodality in oceanic island settings—implications for the petrogenesis of magma in Tenerife, Spain. PhD thesis, University of Dublin, Trinity College

Wiesmaier S, Troll VR, Carracedo JC, Ellam RM, Bindeman I, Wolff JA (2012) Bimodality of lavas in the Teide–Pico Viejo succession in Tenerife—the role of crustal melting in the origin of recent phonolites. J Petrol 53:2465–2495

Wolff JA, Grandy JS, Larson PB (2000) Interaction of mantle-derived magma with island crust? Trace element and oxygen isotope data from the Diego Hernandez Formation, Las Cañadas, Tenerife. J Volcanol Geotherm Res 130:343–366